LANGMUIR

Article

Surface Preconditioning Influences the Antifouling Capabilities of Zwitterionic and Nonionic Polymer Brushes

Ivana Víšová, Marketa Vrabcová, Michala Forinová, Yulia Zhigunová, Vasilii Mironov, Milan Houska, Eva Bittrich, Klaus-Jochen Eichhorn, Hisham Hashim, Petr Schovánek, Alexandr Dejneka, and Hana Vaisocherová - Lísalová

Langmuir, **Just Accepted Manuscript** • DOI: 10.1021/acs.langmuir.0c00996 • Publication Date (Web): 08 Jun 2020

Just Accepted

is published by the American Chemical Society. 1155 Sixteenth Street N.W., Washington, DC 20036

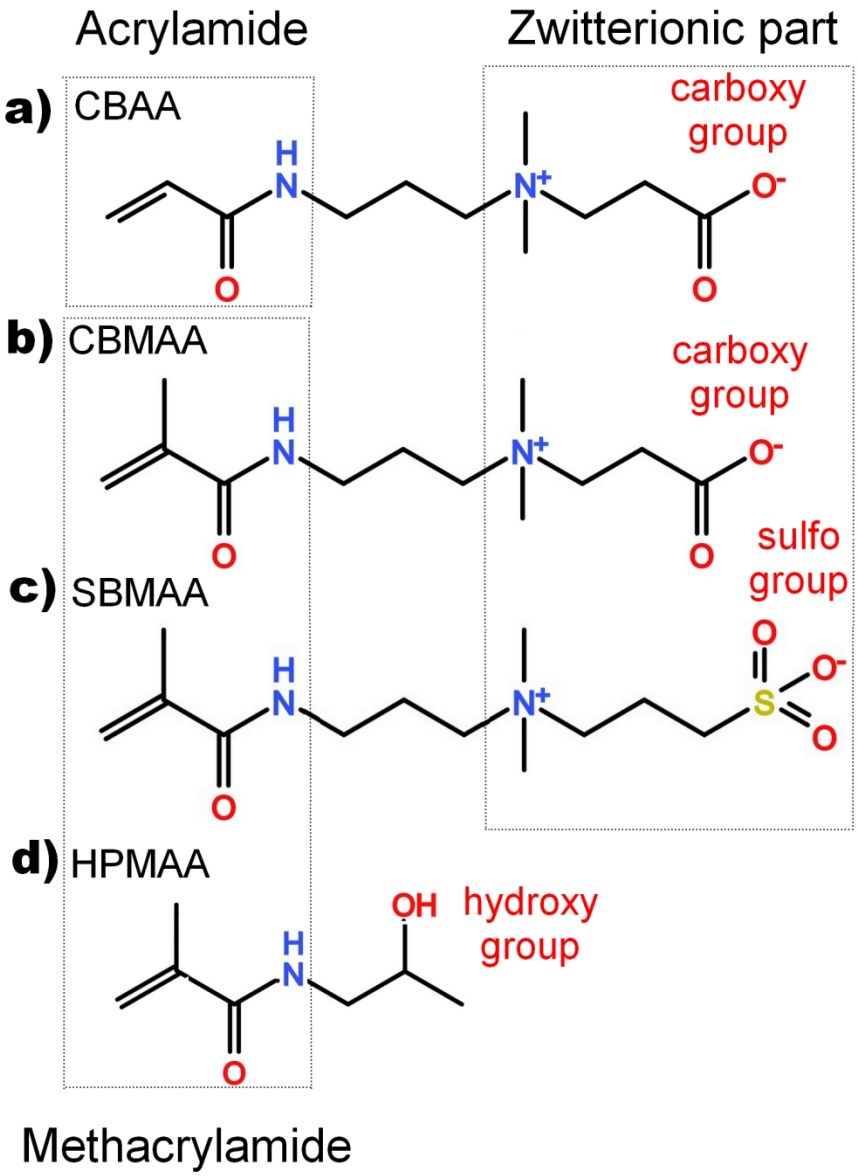

Scheme of monomers used for the polymer coatings used in this study, highlighted with important structure characteristics: we used two zwitterionic carboxy-functionalized monomers, a) carboxybetaine acrylamide (CBAA) and b) carboxybetaine methacrylamide (CBMAA); c) a zwitterionic sulfo-functionalized sulfobetaine methacrylamide (SBMAA), and d) a nonionic N-(2-hydroxypropyl) methacrylamide (HPMAA).

125x168mm (307 x 307 DPI)

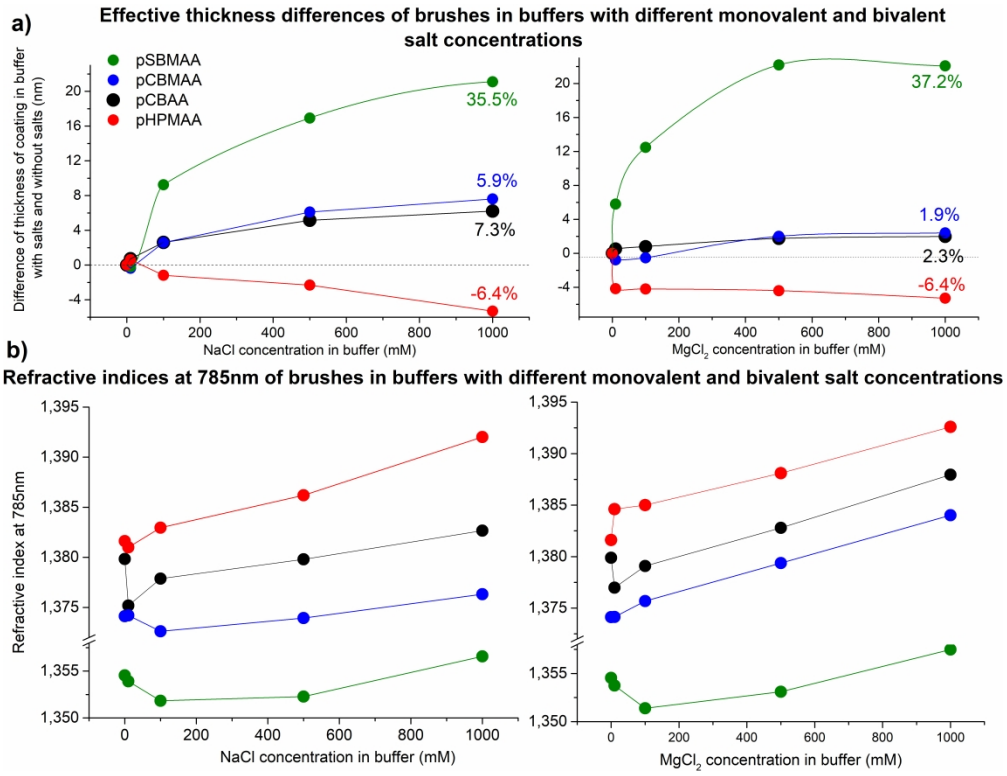

Changes in effective thickness and refractive index (785 nm) of polymer brushes in at varying ionic strength. The effective thickness changes are given as difference between the thicknesses of polymer brushes in buffers with added salts and buffer without added salts. The original thicknesses in buffer without added salts were 86 nm for pCBAA, 129 nm for pCBMAA, 60 nm for pSBMAA, and 82 nm for pHPMAA.

272x208mm (600 x 600 DPI)

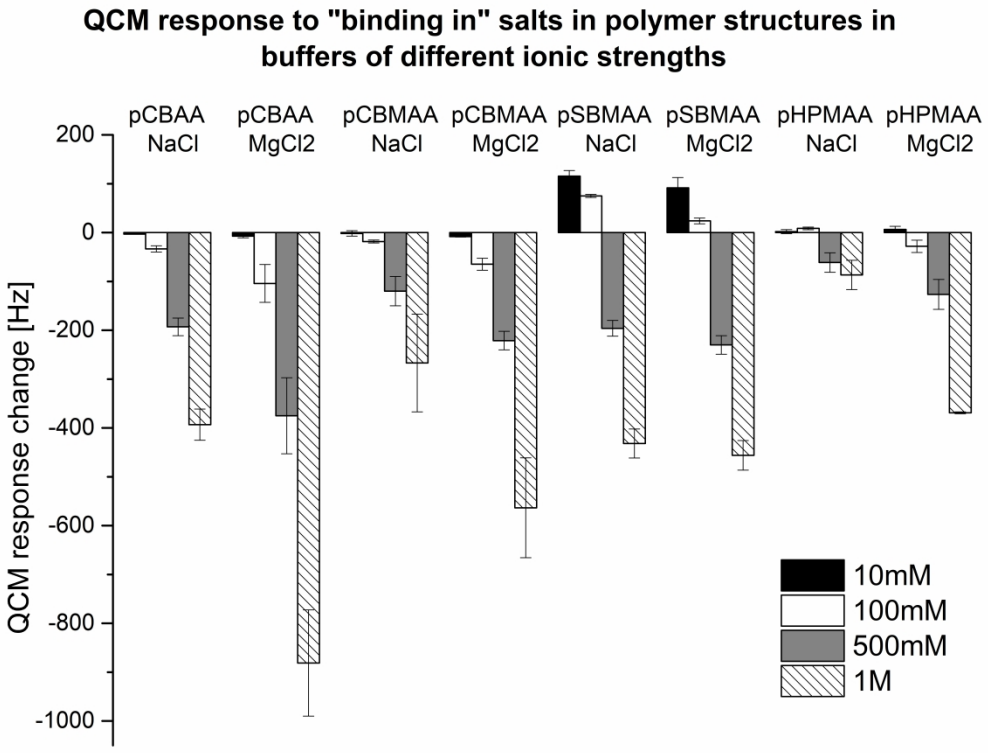

QCM response changes of polymer brush coated quartz crystals in different ionic strength environments with respect to buffer without additional salts

272x208mm (600 x 600 DPI)

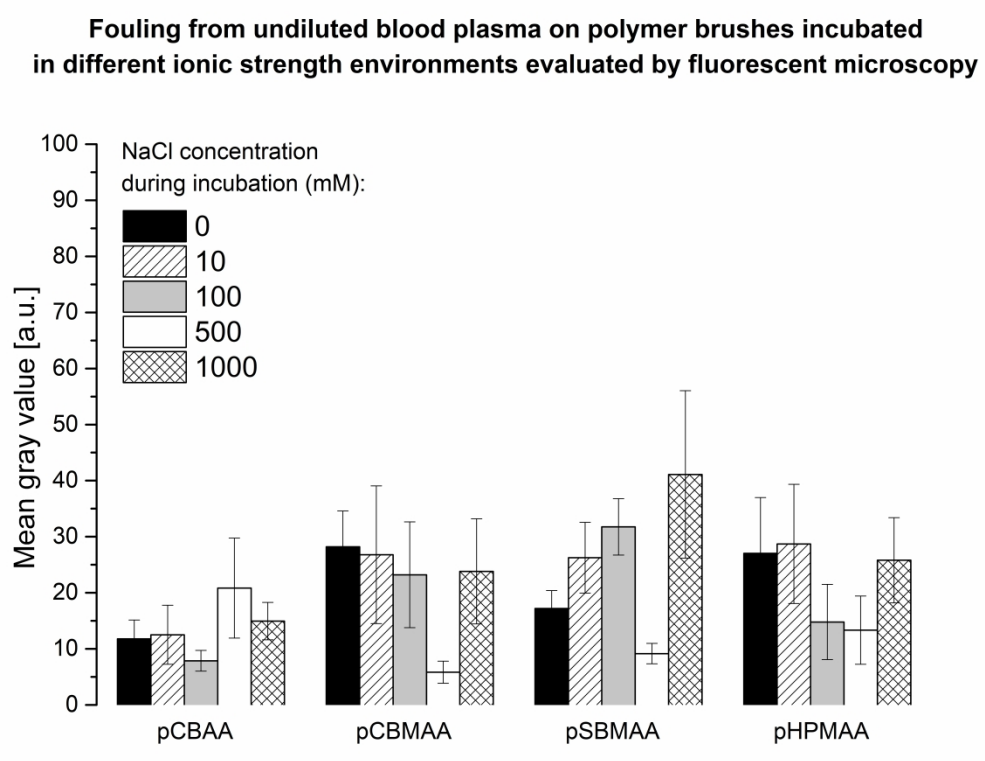

Data from fluorescent microscopy measurements for the fouling resistance to undiluted human blood plasma of different polymer brushes incubated (before exposure to plasma) in buffers with different NaCl concentrations.

272x208mm (600 x 600 DPI)

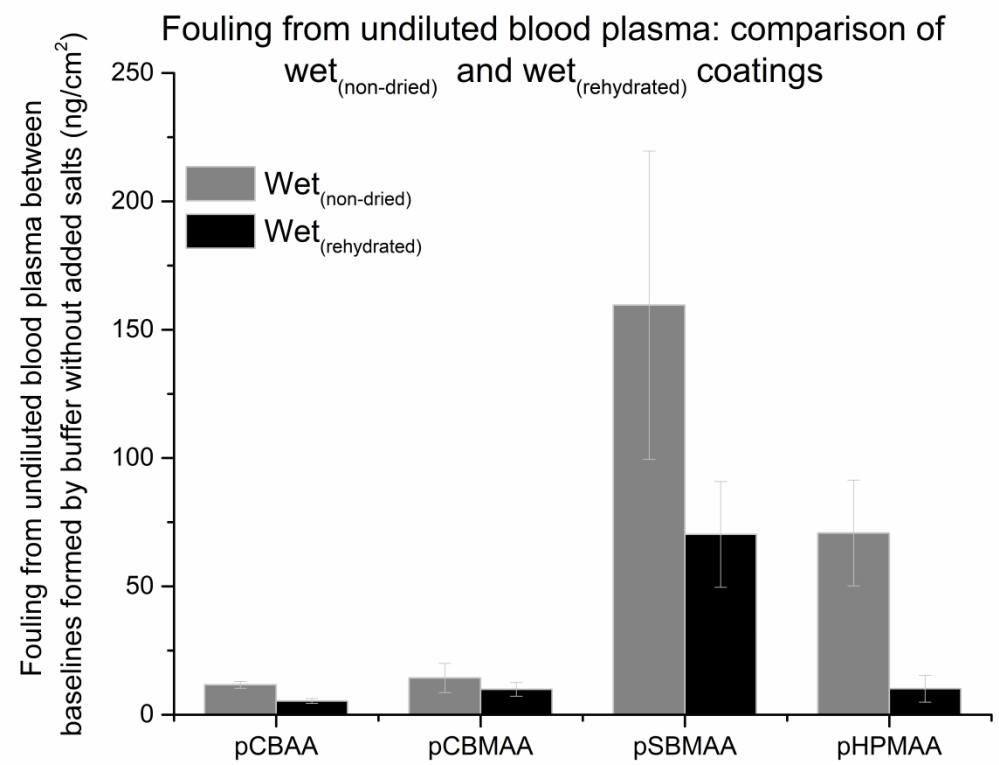

Comparison of the fouling level from undiluted blood plasma on wet(non-dried) and on wet(rehydrated) polymer coatings.

272x208mm (600 x 600 DPI)

Surface Preconditioning Influences the Antifouling Capabilities of Zwitterionic and Nonionic Polymer Brushes

Ivana Víšová[1], Markéta Vrabcová[1], Michala Forinová[1], Yulia Zhigunová[1], Vasilii Mironov[1], Milan Houska[1], Eva Bittrich[2], Klaus-Jochen Eichhorn[2], Hisham Hashim[3,4], Petr Schovánek[1,5], Alexandr Dejneka[1], Hana Vaisocherová - Lísalová[1]

[1] FZU – Institute of Physics of the Czech Academy of Sciences, Na Slovance 1, Prague, Czech Republic.

[2] Leibniz-Institut für Polymerforschung Dresden e.V., Hohe Str. 6, 01069 Dresden, Germany.

[3] National University of Science and Technology (MISIS), Leninskiy prospekt 2, Moscow, 119049, Russia.

[4] Tanta University, Faculty of science, Al-Geish street, Tanta, 31527, Egypt.

[5] Palacký University Olomouc, 17. listopadu 12, 77146 Olomouc, Czech Republic.

Corresponding Author: Hana Vaisocherová-Lísalová, Ph.D., Institute of Physics, Academy of Sciences of the Czech Republic, v.v.i., Na Slovance 1, 18221 Prague, Czech Republic; Tel.: +420 266 05 29 93, E-mail: lisalova@fzu.cz,

Key words: *surface modification, zwitterionic, antifouling functionalizable polymer brush, resistance to fouling, spectroscopic ellipsometry, surface probing*

Abstract

Polymer brushes represent not only emerging surface platforms for numerous bioanalytical and biological applications but also create advanced surface-tethered systems to mimic real-life biological processes. In particular, zwitterionic and nonionic polymer brushes have been intensively studied due to their extraordinary resistance to non-specific adsorption of biomolecules (antifouling characteristics) as well as the ability to be functionalized with bioactive molecules. However, the relation between antifouling behavior in real-world biological media and structural changes of polymer brushes induced by surface preconditioning in different environments remains unexplored. In this work, we use multiple methods to study the structural properties of numerous brushes under variable ionic concentrations and determine the impact of these changes on resistance to fouling from undiluted blood plasma. We describe different mechanisms of swelling, depending on both the polymer brush coating properties and the environmental conditions that affect changes in both hydration levels and thickness. Using both fluorescent and SPR methods, we found that the antifouling behavior of these brushes is strongly dependent on aforementioned structural changes. Moreover, preconditioning of the brush coatings (incubation at a variable salt concentration or drying) prior to biomolecule interaction may significantly improve the antifouling performance. These results suggest a new simple approach to improve the antifouling behavior of polymer brushes. In addition, the results herein enhance the understanding for improved design of antifouling and bioresponsive brushes employed in biosensor and biomimetic applications.

1. Introduction

Surface grafted polymer brushes, i.e. thin polymer films covalently tethered via one end to a substrate, represent a powerful tool for the design of advanced functional surfaces.[1] Aided by advances in surface-initiated polymerization techniques, the molecular structure of a polymer brush can be fine-tuned in composition and density, where brushes with a varying degree of biochemical functionality can be created on many types of surfaces, with areas ranging from ~10cm^2 down to the nanometer scale.[2] In addition to its functionality, these techniques allow for a high degree of control over the physical and chemical characteristics of a material's surface [3, 4].

One tremendously promising use of polymer brushes lies in the development of antifouling coatings, i.e., surfaces that inhibit the non-specific deposition of biological material [5, 6, 7, 8]. Such undesirable fouling, caused by exposure to complex media having the unknown composition (e.g., blood serum and plasma), can inhibit the surface functionality and potentially lead to its failure. Many applications in biology and bioanalytical sciences involve the exposure of a surface to complex media, and antifouling coatings are now an essential component for many applications, including biosensors and analytical methods,[9] tissue engineering,[10] medical implants,[11] drug delivery,[12] and cell culture[13].

Among the previously developed antifouling surfaces, zwitterionic polymer brushes are perhaps the most versatile, especially when used in biorecognition platforms for the analysis of biological media. [3, 6, 14, 15, 16] In addition to having antifouling capabilities, zwitterionic polymer brushes are biocompatible, highly hydratable, have long term stability, and provide high biorecognition element loading capacity. [17, 18, 19, 20]

Among other factors, there are two key structural parameters that are closely linked to the antifouling capabilities of a polymer brush: the brush's hydration capabilities, and its thickness [6, 21, 22, 23]. It has been shown that the fouling resistance of a polymer brush will increase with increases in the brush's hydration level,[24, 25] where tightly bound water molecules in the coating present an extra energy barrier for other molecules to be adsorbed. In addition, many studies have shown that fouling resistance increases with increasing brush thickness;[26] however, the bulk of previous data supporting this claim regard measurements of the dried brush thickness.[17, 27] Highly hydratable coatings can exhibit a remarkable degree of swelling (the thickness change from a dry to wet state),[28] and as shown in the data herein, small differences in a brush's monomer component can lead to substantial differences in swelling. Therefore, for effective comparison of different brushes, it is necessary to consider the brush thickness in a liquid environment.

It is clear that when exposed to the complex nature of a real-world environment, an antifouling coating can be exposed to a variety of physical and chemical conditions, including changes in pH, ionic concentration and type, environment viscosity, and enzymatic activity. Several studies have shown that such changes in environmental conditions can modify fundamental properties of a polymer brush, but only a few studies focused particularly on zwitterionic polymers[29]. Leng et al. demonstrated that hydration levels of zwitterionic polymer brushes were affected by several environmental parameters, including ionic strength, ionic size, charge, and pH.[30] Zhang et al. studied fouling resistance changes of poly(carboxybetaine acrylamide) (pCBAA) in different salt and pH environments on single protein solution, no complex biological media were employed. Yang et al. synthesized a switchable antifouling polymer (poly(3-(1-(4-vinylbenzyl)-1H-imidazol-3-ium-3-yl)propane-1-sulfonate)) and demonstrated its antifouling properties in different salt environments using undiluted blood plasma.[31] Clearly, it is expected that due to strongly adaptive brush behavior environmental changes will lead to changes in the polymer brush structures resulting in affecting the antifouling properties. However, it is rather difficult to completely assess such complex relationships based on existing studies dealing with either single coating types or perform only limited fouling resistance characterization using single protein solutions instead of complex biological media. Therefore, a thorough understanding of these interrelated mechanisms remains unclear and needs to be explored using a broader set of antifouling brush structures.

In this work, we pursue an extensive research on the effects of structural changes of a set of antifouling zwitterionic and nonionic polymer brushes on surface resistance to fouling from undiluted blood plasma using a combination of ellipsometric, quartz crystal microbalance (QCM), fluorescence, and surface plasmon resonance (SPR) data. The structural changes were induced by surface preconditioning in various environmental conditions including distinct salt concentrations and surface drying/rehydrating. The polymer brushes we used (Figure 1) include the carboxy-functional zwitterionic pCBAA and poly(carboxybetaine methacrylamide) (pCBMAA), sulfo-functional zwitterionic poly(sulfobetaine methacrylamide) (pSBMAA), and the nonionic hydroxyl-functional poly(N-(2-hydroxypropyl) methacrylamide) (pHPMAA). This series of antifouling coatings were selected to provide a representative set of antifouling and functionalizable homopolymer brushes with comparable architectures, varying in monomer structures (mostly in functional groups), hence providing a representative set of different surface physicochemical properties.

Specifically, we demonstrate the influence of the ionic strength of the environmental solution on the physical properties of each polymer brush coating, including wet thickness, hydration, and swelling leading to a significant change of antifouling properties. We show that the antifouling properties of zwitterionic and nonionic brushes are strongly influenced by distinct hydration mechanisms. Specifically, based on data taken from both ellipsometry and QCM measurements, we present a hypothesis regarding the mechanism of hydration for each coating. The effect of monovalent and bivalent ions is discussed. In combination with SPR and fluorescence measurements, we relate our results on structural changes to fouling studies using undiluted blood plasma. Finally, discussing an important practical aspect, we compare the effects of drying and rehydrating each coating on their antifouling properties.

2. Experimental section

2.1 Reagents

We used ultrapure Millipore Q water (18.0 MΩ.cm, Milli-Q) for buffer preparation, measurements in water, and all washing steps. HEPES (4-(2-hydroxyethyl)-1-piperazineethanesulfonic acid, hereafter called buffer), 1,4,8,11-tetramethyl-1,4,8,11-tetraazacyclotetradecane (Me4Cyclam, 98%), phosphate-buffered saline (PBS, 0.01 M phosphate, 0.138 M sodium chloride, 0.0027 M potassium chloride), NaCl, $MgCl_2$, CuCl (≥ 99.995%), $CuCl_2$ (99.999%) and methanol (≥ 99.9%) were from Sigma-Aldrich, Czech Republic. The initiator ω-mercaptoundecylbromoisobutyrate was from Prochimia, Poland. Carboxybetaine acrylamide, carboxybetaine methacrylamide, N-(2-hydroxypropyl) methacrylamide, and sulfobetain methacrylamide monomers were from Specific Polymers, France. Tetrahydrofuran (THF, purity ≥99.9%) and ethanol (purity of 96%) were from Penta, Czech Republic. Alexa FluorTM 568 Protein Labeling Kit was from Thermo Fischer Scientific, USA. QCM crystals with evaporated gold layer were from Krystaly, Czech Republic. The human blood plasma (pooled, mixed gender) in sodium citrate was from VWR International, Czech Republic.

2.2 Polymer brush coating preparation

Polymer brushes were prepared by surface-initiated atom transfer radical polymerization (SI-ATRP) using an optimized procedure and a custom-made polymerization system developed in house. More details are presented in the Supporting information. The monomers used in the polymerization for each brush are shown in Figure 1.

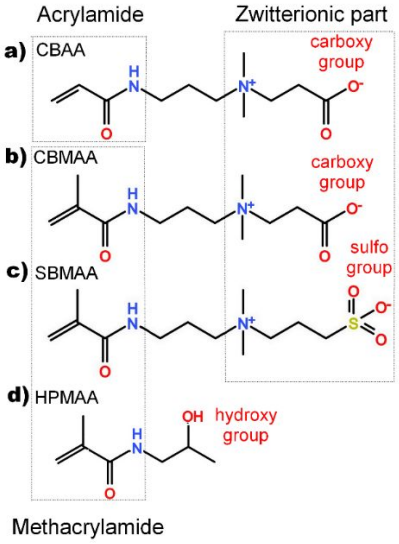

Figure 1: Scheme of monomers used for the polymer coatings used in this study, highlighted with important structure characteristics: we used two zwitterionic carboxy-functionalized monomers, **a)** carboxybetaine acrylamide (CBAA) and **b)** carboxybetaine methacrylamide (CBMAA); **c)** a zwitterionic sulfo-functionalized sulfobetaine methacrylamide (SBMAA), and **d)** a nonionic *N*-(2-hydroxypropyl) methacrylamide (HPMAA).

2.3 Refractometric measurements of buffers

All solutions used in this study were prepared in stock and their optical constants were characterized by a digital multi-wavelength refractometer (DSR-λ, Schmidt + Haensch GmbH & Co., Berlin, Germany) measured at room temperature (25 °C). For each solution (water, buffer, buffer with added salts) we measured the RI at 6 different wavelengths. After, these data were extrapolated in the full region of 350 – 800nm, taking into account the standard dispersion function of water. Experimental measurements for all solutions, along with fitted (and extrapolated) RI data, are shown in Figure S2 in the Supporting information.

2.4 Spectroscopic ellipsometry and QCM in liquid environments

Ellipsometry is a sensitive surface technique that, when combined with an appropriate modeling procedure, can accurately measure several characteristic parameters of thin polymer brush films, including effective thickness, refractive index (RI), layer density, surface roughness, and relative structural composition.[32] In this work, ellipsometric measurements were performed using a spectroscopic ellipsometer (VASE, J.A.Woollam, Lincoln, USA) in the spectral range of 3.4 – 1.5 eV with steps of 0.008 eV and a 70° incidence angle. Measurements were taken at room temperature using a custom-made cell (covered to prevent water evaporation) having an incorporated sample holder to ensure that all data were taken from the same sample spot across all used liquids (Figure S1, more details in Supporting information). For a reference, we used a bare Au-coated BK7 glass chip from the same batch as the substrates used for polymer coating.

Data analysis was performed with WVASE32 software. Experimental data were fitted with a single- or double-oscillator model (variety of Gaussian and Tauc-Lorentz oscillators), depending on the brush. Model fitting to experimental data with the fits of thickness uniqueness is shown in Figure S3 in the Supporting information.

QCM measurements were performed at room temperature using a custom-made two-channel apparatus consisting of portable QCM Analyzer (KEVA, Brno, Czech Republic) and a microfluidic-based crystal holder, previously described in detail.[33] Au-coated QCM crystals with the resistance of max. 30 Ω and frequency range around 10000 kHz were used for polymer-brush coated sensor preparation.

More details about QCM and ellipsometric measurements are provided in the Supporting information.

2.5 Fouling resistance studies by fluorescent microscopy

Coatings from the same batches as those used for ellipsometric studies were immersed in buffer with different concentrations of sodium chloride (0-1000 mM) for 20 minutes. This incubation time was found to be long enough to complete the surface response to environmental changes as confirmed by spectroscopic ellipsometry (data not shown). Afterward, undiluted human plasma was applied for 10 minutes and then chips were washed with plain buffer (to avoid the electrostatically induced loss of nonspecifically deposited material). The plasma incubation time of 10 minutes was selected as it corresponds to a typical detection time used in biosensor applications [34]. All substrates were then labeled with Alexa Fluor 568 using the Alexa FluorTM 568 Protein Labeling Kit. Labeled samples were then imaged using a high-resolution spinning disk confocal microscope (Spin SR, Olympus), using the acquisition software cellSens (Olympus, Tokyo, Japan), and processed using ImageJ (NIH). For each polymer type we measured mean grey values on 30 areas at random positions; this value is proportional to the nonspecifically adsorbed amount of protein (i.e., fouling) on each surface.

2.6 Fouling resistance studies by SPR

SPR fouling studies were performed on an angular MP-SPR with a 4-channel microfluidic system, equipped with LED sources of 670 nm and 785 nm wavelengths (BioNavis Ltd, Finland). To transform angular units (corresponding to a shift in the SPR resonance angle) to mass units of proteins adsorbed on the surface, we used a value of 0.001° = 0.85 ng/cm^2 (785 nm). More details on the SPR experiments are provided in the Supporting information.

3. Results and discussion

3.1 Probing hydrated polymer brush structures by spectroscopic ellipsometry and QCM

The spectroscopic ellipsometry was employed to study 4 different antifouling hydrophilic polymer brush coatings in different ionic strength liquid environments. The monomers for these polymers are shown in Figure 1: the structures of carboxy-functional pCBAA and pCBMAA differ only in the presence of a methyl group in the backbone; the permanent negative charge of pSBMAA is given by a sulfo-group (more polar than the carboxy-group), and the nonionic pHPMAA bearing hydroxyl groups is uncharged (Figure 1). The spectral characteristics of all prepared polymers were measured by infrared spectroscopy (Figure S5).

To provide reliable ellipsometry characteristics of polymer brushes, accurate model input parameters are an absolute prerequisite for reliable calculation of these parameters, especially regarding highly hydratable polymer brush structures.[28] Therefore, all solutions that were used in a polymer brush environment were prepared in stock and characterized by refractometric measurements prior to ellipsometric data processing. Additionally, the hardware was optimized to ensure accurate measurements, the details of which can be found in the Supporting information.

Previous work has typically used either the Cauchy or Cauchy-Urbach models for fitting data regarding dielectric molecular layers of polymer structures.[35, 36, 37, 38] Conversely, for the more complex zwitterionic brushes used herein, the simple parameters of these models were not found to be sufficient for a best-fit across all measured wavelengths. Moreover, we found that no universal fitting model was sufficient when used alone. Therefore, in order to reflect all the potential differences in brush architectures and thus reliably perform ellipsometric data analysis, we optimized the fitting model for each type of brush structure. Specifically, we used a single-oscillator (Tauc-Lorentz) model for pCBAA and pSBMAA brushes, and a double-oscillator (Gaussians) model for pCBMAA and pHPMA brushes. Further details on experimental procedures, as well as example spectra (Figure S3), can be found in the Supporting information.

All of the brushes in this study had a wet thickness between 60-130 nm, for which we used the above-mentioned oscillators for data analysis. To characterize the structure in more detail, we prepared a set of thicker pCBAA brushes (206-242 nm). Ellipsometric analysis of these brushes (using a graded layer oscillator model) revealed a gradient RI profile, where the measured RI decreased monotonically away from the surface (Figure S4, Supporting information). As RI correlates with the density of the polymer brush, these results suggest that these brushes have a pseudo-ordered

structure, where the level of structure periodicity is higher near the gold surface (with polymer chains fixed to the initiator layer), and diminished towards the brush/water blurred interface. More information and all measured spectra can be found in the Supporting information.

To gain insight into the inner structure of the hydrated polymer brushes, the samples were exposed to HEPES buffer with different concentrations of added monovalent and bivalent chloride salts. Other buffer parameters (pH 7.4 - physiological pH of normal arterial blood, 25° C – room temperature) were kept constant.

We monitored changes in the effective thickness and refractive index using fits to data collected by spectroscopic ellipsometry; this data is shown in Figure 2 for all four polymer brushes. Data for the %-increase is shown for the 1M data, calculated from the thickness measured in buffer with no added salts. For better clarity, Figure 2 shows refractive indices only for a wavelength of 785 nm (the wavelength used in SPR experiments); the total set of the refractive index spectra for wavelengths from 350- 850nm can be found in the Figure S6 in the Supporting information.

With increasing ionic strength, all zwitterionic coatings exhibit an increase in effective thickness, whereas the effective thickness of nonionic pHPMAA systematically decreases. The pCBAA and pCBMAA brushes exhibited an increase in effective thicknesses of 7.3% and 5.9% in 1M NaCl, with shorter increases of 2.3% and 1.9% in 1M MgCl2, respectively. In comparison, thickness increases for pSBMAA were 5-6 times higher for NaCl and 15-times higher for MgCl2 (35.5% and 37.2%, respectively).

For carboxy-functional zwitterionic coatings (pCBAA, pCBMAA), increases in effective thickness were about 3 times higher in NaCl than in MgCl2 solutions, indicating a higher response of both structures to the concentration of monovalent compared to bivalent salt ions. On the other hand, the thicknesses of both pHPMAA and pSBMAA brushes were only weakly affected by ion type. The response to ionic concentration was most significant for pSBMAA compared to other polymer brushes.

In higher ionic strength environments, all of the zwitterionic brushes had increased thickness with increasing salt concentration, which was accompanied by increases in the refractive index (Figure 2b, Figure S6). These results suggest that at higher ionic strength, a portion of the water molecules in the inner zwitterionic brush structure is substituted or appended with salt-based counterions, ordering themselves around charged groups inside the brush structure and shielding internal electrostatic interactions among chains. This is consistent with prior research, where Leng et al. showed that SFG (sum frequency generation vibrational spectroscopy) water signals in zwitterionic polymers decreased with increasing NaCl concentration,[30] indicating the disruption of water molecule ordering and increasing amounts of ions binding to the polymers. Hence, zwitterionic brushes will tend to grow thicker and optically denser due to changes in electrostatic interactions between polymer chains and salt ions, redistribution of water bonds, and changes in ambient composition within the polymer structure (Figure S9). On the other hand, non-ionic pHPMAA showed systematic decrease in thickness and increase in refractive index with increasing salt concentration. Such shrinking suggests different swelling mechanism, incorporating mostly rearrangement of water molecules within the structure and dehydration.

Looking at detailed differences in pCBAA and pCBMAA responses to different ionic strength environments, we can observe a slightly lower tendency for pCBMAA to grow thicker with increasing salt concentration. pCBAA in 1M NaCl environment exhibits 1.2 times higher thickness increase compared to pCBMAA (similar results for MgCl2). We assume that this effect can be caused by the extra methyl group, i.e., increased hydrophobicity of the pCBMAA backbone structure, which might bring higher spatial stability and rigidity to the whole brush architecture. In addition, a different affinity of salt ions to methacrylamide compared to acrylamide backbone can be expected. As discussed later, the QCM data in Figure 3 support this hypothesis, showing a slightly lower amount of both salt ion types bound in the pCBMAA structure compared to the pCBAA.

In pSBMAA, the increment to thickness is up to an order of magnitude higher than the carboxy-group terminated polymers; perhaps caused by the higher polarity of the sulfo-groups in comparison to carboxy-groups. There might also be a remarkable influence on packing density: the pSBMAA shows a significantly lower refractive index than carboxy-terminated brushes (Figure 2b, Figure S6), suggesting a significantly lower packing density of pSBMAA compared to all studied zwitterionic coatings. Taking into account higher swelling ratio (Table 1) and lower refractive index (Figure 2b), we hypothesize that instead of being grafted densely, pSBMAA seems to contain longer chains bundled tightly at lower salt ion concentrations, and loosening at higher salt ion concentrations when electrostatic interactions between the chains are screened by a higher ionic strength environment.

In all zwitterionic structures, there is a clear dip in the refractive index in the region of 10-100 mM for both monovalent and divalent salt ion concentrations (Figure 2b and Figure S6) accompanied by systematical increase of the brush thickness. We assume that this dip is related to two competitive processes occurring in the structure during swelling. In particular, it is anticipated that the zwitterionic coatings occupy an equilibrium layout in buffer solution without added salts. Upon increasing ionic strength, electrostatic interactions between the chains become screened by salt counterions and the structure becomes loosened: the refractive index decreases while the thickness grows. When the concentration

of salt ions reaches a threshold value, the binding of counterions into the brush structure starts to compensate for refractive index drops caused by loosening of polymer chains, and the refractive index starts to increase.

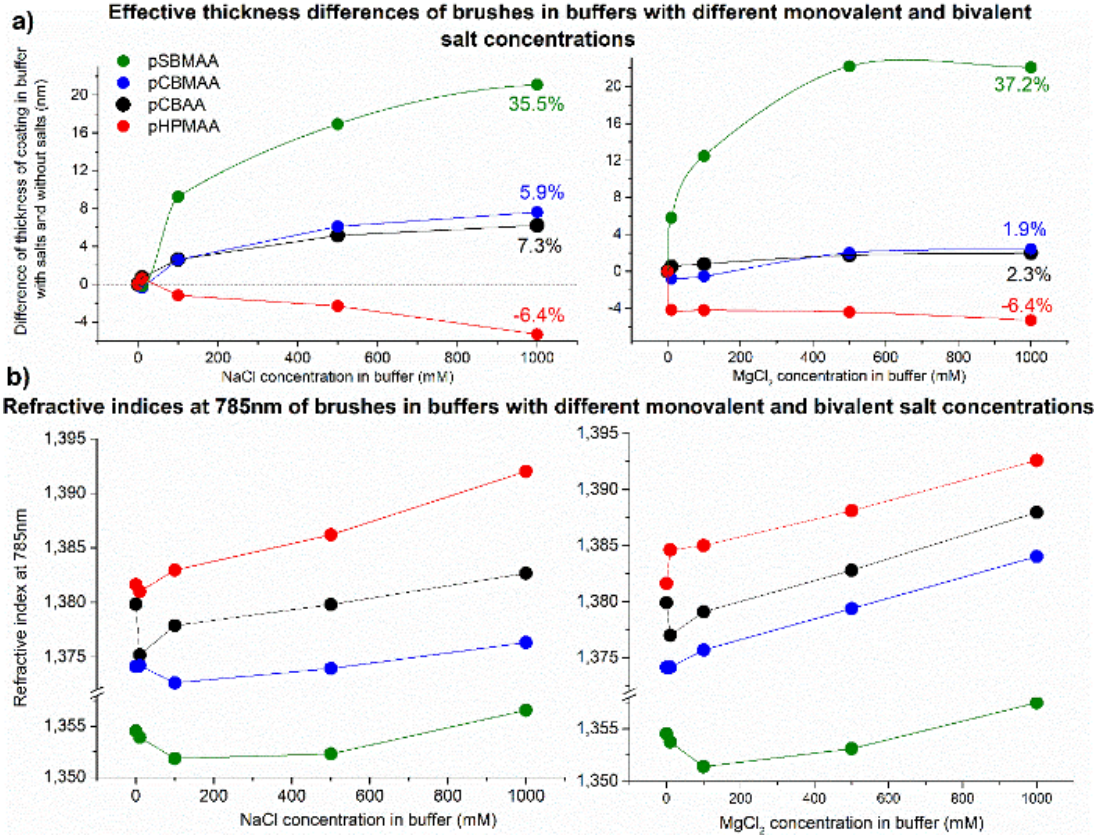

Figure 2: Changes in effective thickness and refractive index (785 nm) of polymer brushes in at varying ionic strength. The effective thickness changes are given as difference between the thicknesses of polymer brushes in buffers with added salts and buffer without added salts. The original thicknesses in buffer without added salts were 86 nm for pCBAA, 129 nm for pCBMAA, 60 nm for pSBMAA, and 82 nm for pHPMAA.

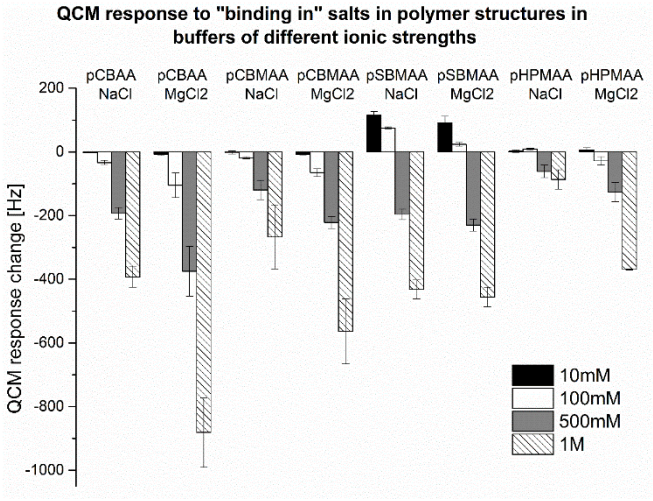

Figure 3: QCM response changes of polymer brush coated quartz crystals in different ionic strength environments with respect to buffer without additional salts.

We performed additional QCM experiments to further confirm the hypothesis about increasing salt concentration in brush structures at higher ionic strengths. In contrast to ellipsometry or SPR, QCM is insensitive to refractive index changes. Rather, changes in the QCM response are related to the mass of salt ions bound in the polymer brush structure, the amount of water repelled from the structure, and changes in viscosity of area around the crystal surface (related to the degree of swelling).

A trend of decreasing QCM frequency with increasing ionic strength was observed for all studied types of polymer brushes, suggesting an increasing mass of the salt ions bound to the polymer structures with increasing ionic strength. For all salt concentrations in all samples, the sensor response decrease for MgCl2 is greater or equal to NaCl. Taking into account that the molecular weight of the MgCl2 molecule is 1.6 times higher than that for NaCl, similar affinities to monovalent and bivalent salt ions were observed for carboxybetaines. Conversely, in pSBMAA the responses are nearly equal, suggesting a higher affinity of the coating to NaCl. The opposite trend was observed in pHPMAA, where the affinity to MgCl2 seems to be slightly higher than NaCl (1M data).

The combination of results shown in Figure 3 with the dry thicknesses of coatings (Table 1) suggests that a significantly lower amount of salt ions was bound in the pHPMAA brush (normalized by dry thickness) in comparison with any zwitterionic brushes. This is in line with the hypothesis of different swelling mechanisms for zwitterionic and nonionic structures. In particular, a decrease of pHPMAA thickness with increasing ionic strength is related mostly to dehydration; only a limited amount of salt ions is attached to the structure. For the zwitterionic brushes, the increase of thickness (with increasing ionic strength) is strongly associated with an increasing amount of salt ions bound in the polymer brush coating.

Interestingly, we observed an increase in the QCM response for pSBMAA for both 10 mM and 100 mM salt ion concentrations (Figure 3). We suggest that this effect is connected with the previously described lower pSBMAA packing density and its dynamics in an ionic environment. Pertaining to the rapid change in brush thickness ($\leq$ 100 mM) in solutions of both salts (Figure 2a): with no added salts the polymer chains are likely more coil-like near the crystal surface, and at 10 mM the chains start to uncoil, transferring some mass away from the crystal surface. As the ionic strength of 10 mM salt is relatively low, the effect of binding salt ions in the structure cannot counterweight the effect of chains straightening, and the QCM signal increases. Above 100 mM the effects are equal and with higher ionic strength, salt ions binding starts to predominate. This explanation is supported also by Figure 2b, where a decrease of the refractive index from 0-100 mM ("unbounding") can be seen, with further increases in ionic strength the refractive index starts to increase (as salt ions become bound into the structure).

3.2 Fouling resistance to undiluted blood plasma influenced by preconditioning of brushes at different salt concentrations

The fluorescent microscopy was employed to assess the influence of the structural changes of brushes exposed to different salt concentrations (i.e., preconditioning) on the fouling resistance. This method possesses a sensitivity independent of any thickness changes of the brush coating, including those induced by the changes in the surrounding environment. The results of these experiments (Figure 4, Figure S8) show that fouling resistance of the polymer brushes studied herein is strongly influenced by structural changes caused by preconditioning of the coatings in NaCl solutions with different ionic strengths. Differences between acrylamide and methacrylamide based coatings can be observed. The optimum concentration of NaCl in the brush environment before injection of undiluted plasma to achieve a maximum surface fouling resistance was found to be 500 mM NaCl for all methacrylamide-based brushes. On the other hand, the optimum NaCl concentration for the acrylamide-based brush was 100 mM, with fouling that is comparable with the lowest level achieved by the methacrylamide brushes. These data may help to optimize the preconditioning of the coatings to achieve better fouling resistances. It is noteworthy, though, that the optimum NaCl concentrations may differ for some types of polymer brushes from physiological levels (ca. 0.15 M).

Zhang et al. observed that protein adsorption to pCBAA tends to decrease in a higher ionic strength environment;[39] however, that study was performed with single protein solutions and more importantly, the salts were also present in the buffer during the fouling measurement. Hence, electrostatic interactions could have been shielded by higher ionic strengths, leading to a decrease of non-specific bindings. Moreover, theoretic predictions indicate that polymeric zwitterions tend to become more hydrated as the NaCl concentration of the environment increases.[22] Nevertheless, it is difficult to straightforwardly apply these findings from these valuable studies for coatings employed in direct contact with real-world biological samples, in which the salt concentrations are fixed. Here, we use the different salt concentration environments prior to plasma injections for brush preconditioning to achieve a specific hydrated structure of the polymer brush.

In summary, compared to previous works, we attempted to provide an extensive study comprising different classes of antifouling monomers on the complex relationships between antifouling properties and environment-induced structural

changes of polymer brushes. Based on such a study, more generalized observations highlighting the differences in zwitterionic and nonionic brush adaptive behavior were determined. For example, we found that relatively small changes in brush thickness (usually lower than 10%) induced by salt concentration changes in a surrounding environment led to significant changes in antifouling properties. For instance, plasma fouling observed for pCBMAA after pre-incubation in 500 mM NaCl was 5 times lower than the plasma fouling after pre-incubation in 0mM NaCl. Moreover, remarkable difference in environment-induced antifouling behavior between pCBAA and pCBMAA brushes composed of monomers having a very similar structure (differing only in a presence of methyl in a methacrylamide backbone of pCBMAA, Figure 1) was observed. While for pCBAA the optimum NaCl concentration giving the maximum fouling resistance was 100mM, which is close to physiological conditions, in the case of pCBMAA (and all other studied methacrylamide based coatings) the optimum value was much higher, i.e. 500mM NaCl.

It is worth mentioning that in this work, we focus on the initial phase of brush response to surface preconditioning. We assume that this phase is a critical part of the whole fouling process. Therefore, relatively short blood plasma incubation time (10 minutes) was employed herein. Moreover, this incubation time is relevant for many biosensor applications, which tend to perform rather a rapid analyte detection. A detailed study on the complex phenomena of fouling dynamics is a subject of our further work.

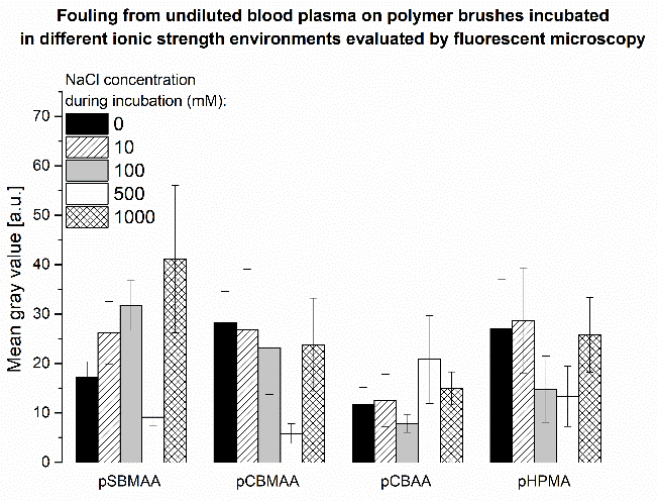

Figure 4: Data from fluorescent microscopy measurements for the fouling resistance to undiluted human blood plasma of different polymer brushes incubated (before exposure to plasma) in buffers with different NaCl concentrations.

3.3 Reversibility of hydration and impact of drying on fouling resistance

We used both spectroscopic ellipsometry and SPR to investigate the ability of polymer brushes to recover their properties after rehydration. Here we used the SPR method for fouling resistance measurements, as it is considered to be a standard method for fouling evaluation. Moreover, for these experiments the HEPES buffer with no added salts was used, thus we expected no changes in swelling in each polymer brush (that might interfere with measured data).

We used ellipsometry to measure the effective thickness and refractive index of wet brushes that have not been dried ($wet_{non\text{-}dried}$), dried brushes, and rehydrated brushes ($wet_{rehydrated}$); these results are shown in Table 1. All coatings exhibited a slight increase in effective thickness after rehydration. The extra methyl group in the pCBMAA structure may bring some differences in recovery after drying, as pCBAA shows two times higher relative increase in rehydrated effective thickness than pCBMAA (5.5%, 2.4% respectively). The relative thickness increase of pSBMAA (by 9.2%) is the highest of all studied zwitterionic coatings. Nonionic pHPMAA changes its thickness only by 3.9%.

The swelling, expressed as the ratio of effective thickness of $wet_{rehydrated}$ and wet_{dried} (Table 1), is the lowest for pHPMAA: from a dry state to a rehydrated, effective thickness increased by a factor of 1.8. In the case of zwitterionic coatings, this ratio was in the range of 3-4.

Besides the effective thickness increase, all studied coatings exhibited a decrease in the refractive index after being dried and rehydrated; Figure S7 shows the entire RI spectrum for all 4 brushes. pHPMAA shows the largest decrease in the refractive index (0.005) with respect to the other brushes (~0.002).

We hypothesize that drying after polymerization changes the layout of intermolecular forces in the inner structure of a coating. Rehydrated coatings tend to bind more water in their structure than non-dried coatings, leading to the creation

of thicker and more hydrated layers having a larger effective thickness and smaller refractive index. This hypothesis is supported by SPR data, where we compared the fouling resistance of non-dried and rehydrated brushes to undiluted blood plasma. These results, shown in Figure 5, clearly show that fouling levels are considerably lower on rehydrated brushes with respect to non-dried brushes. These findings are consistent with previous literature, where higher levels of hydration are connected with higher fouling resistance.[24, 25, 40].The fouling values for re-hydrated brushes are in line with those reported in a literature [17, 41, 42]. The most significant resistance improvement was seen in pHPMAA brushes, which demonstrated the largest refractive index change (related to the largest relative increase in hydration level after rehydration).

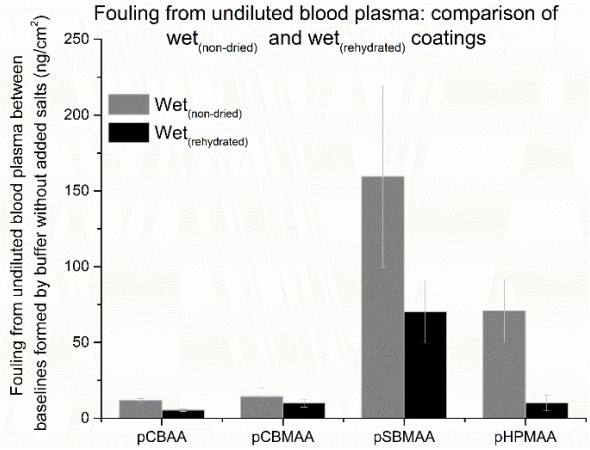

Figure 5: Comparison of the fouling level from undiluted blood plasma on $wet_{(non\text{-}dried)}$ and on $wet_{(rehydrated)}$ polymer coatings.

It should be noted that there is a relative difference (compared to other coatings) between the lower fouling of pSBMAA indicated by fluorescent microscopy (in HEPES without salts, Figure 4) when compared to a rather high value determined by SPR (Figure 5). We believe that this difference may be caused by the differences between the applied methods. A comparison of different methods used to assess the fouling of highly hydratable coatings susceptible to high level of swelling remains the focus of a future study.

Table1: Comparison of effective thickness before drying and after rehydration.

	pCBAA	pCBMAA	pSBMAA	pHPMAA
Effective wet thickness $wet_{non\text{-}dried}$ (nm)	119.0 ± 0.1**	119.2 ± 0.2**	67.3 ± 0.8**	82.5 ± 0.4**
Refractive index $wet_{non\text{-}dried}$	1,376	1,373	1,355	1,383
Effective dry thickness (nm)	39.3 ± 0.5**	38.8 ± 0.4**	16.7 ± 0.1**	47.7 ± 0.2**
Effective wet thickness $wet_{rehydrated}$ (nm)	125.4 ± 0.2**	122.1 ± 0.2**	73.6 ± 1.1**	85.7 ± 0.2**
Refractive index $wet_{rehydrated}$	1,373	1,372	1,353	1,378
Swelling * (%)	319	315	442	180

*Swelling was assessed as percentage of rehydrated effective thickness from dry effective thickness.

**Errors of the effective thicknesses in the table are the errors of parameters given by fit of the ellipsometric data

4. Conclusions

This extensive study revealed a remarkable dependence of antifouling properties of both zwitterionic (pCBAA, pCBMAA, pSBMAA) and nonionic (pHPMAA) polymer brushes on the structural changes induced by the adaptive brush response to ionic strength of their surrounding environment. Using spectroscopic ellipsometry, we observed monotonic increases in thickness of carboxy- and sulfo- functional zwitterionic coatings with increasing ionic strength; however, their refractive index exhibited more complex behavior, which reflected the capture of salt ions, hydration, and the corresponding loosening of the brush chains. On the contrary, nonionic pHPMAA responded to increases in ionic strength by shrinking, which was attributed to dehydration. A series of complementary QCM measurements indicated the same trend of capturing salts for zwitterionic brushes, with much less capture for pHPMAA. The results revealed that brush "preconditioning" at various salt concentrations may improve the antifouling properties by up to 70%; the optimum "preconditioning" parameters providing the highest degree of fouling resistance were determined for each brush type and structure. These results suggest a potential method of how to optimize fouling resistance for practical applications. Another issue important for practice is the ability to store low fouling coatings in a dry state. Rehydration experiments, evaluated by both ellipsometry and SPR, indicated that all brushes exhibited a full recovery, with slightly higher hydration after one drying/rehydration cycle. Correspondingly, all of the brushes exhibited significantly improved fouling resistance from blood plasma after rehydration. The complex responses of antifouling materials to environmental conditions, as shown herein, highlight the importance of an in depth understanding for processes occurring in the brush layers in native environments.

Acknowledgments

This work was supported by Praemium Lumina quaeruntur of the Czech Academy of Sciences (LQ100101902) and by the project of Operational Programme Research, Development and Education of The Ministry of Education, Youth and Sports (CZ.02.1.01/0.0/0.0/17_049/0008422). The authors would like to thank Daniel Špaček for his help with the graphic design, and N. Scott Lynn Jr. and Djamel Eddine Chafai for their insightful comments.

Supporting information description

The supporting information is available and includes: Polymerization procedure, spectroscopic ellipsometry, QCM, and SPR measurements in detail, optimized hardware for ellipsometry in liquid environment, dispersion functions of used liquids, examples of measured and fitted ellipsometric data of polymers, infrared spectra of polymer brushes, influence of different ionic strength of environment on swelling of polymer brushes: refractive index spectra, refractive index change after rehydration in polymer brush structures (pdf).

References

1. Krishnamoorthy, M.; Hakobyan, S.; Ramstedt, M.; Gautrot, J. E. Surface-Initiated Polymer Brushes in the Biomedical Field: Applications in Membrane Science, Biosensing, Cell Culture, Regenerative Medicine and Antibacterial Coatings. *Chemical Reviews* **2014,** *114* (21), 10976-11026.
2. Yan, J.; Bockstaller, M. R.; Matyjaszewski, K. Brush-modified materials: Control of molecular architecture, assembly behavior, properties and applications. *Progress in Polymer Science* **2020,** *100*, 101180.
3. Liu, B.; Liu, X.; Shi, S.; Huang, R.; Su, R.; Qi, W.; He, Z. Design and mechanisms of antifouling materials for surface plasmon resonance sensors. *Acta Biomater* **2016,** *40*, 100-118.
4. Banerjee, I.; Pangule, R. C.; Kane, R. S. Antifouling coatings: recent developments in the design of surfaces that prevent fouling by proteins, bacteria, and marine organisms. *Adv Mater* **2011,** *23* (6), 690-718.
5. Jiang, C.; Wang, G.; Hein, R.; Liu, N.; Luo, X.; Davis, J. J. Antifouling Strategies for Selective In Vitro and In Vivo Sensing. *Chem Rev* **2020,** 120, 3852–3889.
6. Blaszykowski, C.; Sheikh, S.; Thompson, M. A survey of state-of-the-art surface chemistries to minimize fouling from human and animal biofluids. *Biomater Sci* **2015,** *3* (10), 1335-70.
7. Yu, Q.; Zhang, Y.; Wang, H.; Brash, J.; Chen, H. Anti-fouling bioactive surfaces. *Acta Biomater* **2011,** *7* (4), 1550-7.
8. Sun, F.; Hung, H. C.; Sinclair, A.; Zhang, P.; Bai, T.; Galvan, D. D.; Jain, P.; Li, B.; Jiang, S.; Yu, Q. Hierarchical zwitterionic modification of a SERS substrate enables real-time drug monitoring in blood plasma. *Nat Commun* **2016,** *7*, 13437.
9. Zhang;, T.-D.; Zhang;, X.; Deng, X. Applications of protein-resistant polymer and hydrogel coatings on biosensors and biomaterials *Annals of Biotechnology* **2018,** *2,* 1006-1012.
10. Cao, S.; Barcellona, M. N.; Pfeiffer, F.; Bernards, M. T. Tunable multifunctional tissue engineering scaffolds composed of three-component polyampholyte polymers. *Journal of Applied Polymer Science* **2016,** *133* (40), 43985-43994.
11. Lin, P.; Lin, C.-W.; Mansour, R.; Gu, F. Improving biocompatibility by surface modification techniques on implantable bioelectronics. *Biosensors and Bioelectronics* **2013,** *47*, 451-460.
12. Chen, W.; Yung, B. C.; Qian, Z.; Chen, X. Improving long-term subcutaneous drug delivery by regulating material-bioenvironment interaction. *Advanced Drug Delivery Reviews* **2018,** *127*, 20-34.
13. Víšová, I.; Smolková, B.; Uzhytchak, M.; Vrabcová, M.; Zhigunova, Y.; Houska, M.; Surman, F.; de los Santos Pereira, A.; Lunov, O.; Dejneka, A.; Vaisocherová-Lísalová, H. Modulation of Living Cell Behavior with Ultra-Low Fouling Polymer Brush Interfaces. *Macromolecular Bioscience,* **2020**, 20 1900351-.1900359.

14. Zheng, L.; Sundaram, H. S.; Wei, Z.; Li, C.; Yuan, Z. Applications of zwitterionic polymers. *Reactive and Functional Polymers* **2017,** *118*, 51-61.
15. Lísalová, H.; Brynda, E.; Houska, M.; Víšová, I.; Mrkvová, K.; Song, X. C.; Gedeonová, E.; Surman, F.; Riedel, T.; Pop-Georgievski, O.; Homola, J. Ultralow-Fouling Behavior of Biorecognition Coatings Based on Carboxy-Functional Brushes of Zwitterionic Homo- and Copolymers in Blood Plasma: Functionalization Matters. *Analytical Chemistry* **2017,** *89* (6), 3524-3531.
16. Lin, X.; Jain, P.; Wu, K.; Hong, D.; Hung, H. C.; O'Kelly, M. B.; Li, B.; Zhang, P.; Yuan, Z.; Jiang, S. Ultralow Fouling and Functionalizable Surface Chemistry Based on Zwitterionic Carboxybetaine Random Copolymers. *Langmuir* **2019,** *35* (5), 1544-1551.
17. Vaisocherová-Lísalová, H.; Surman, F.; Víšová, I.; Vala, M.; Špringer, T.; Ermini, M. L.; Šípová, H.; Šedivák, P.; Houska, M.; Riedel, T.; Pop-Georgievski, O.; Brynda, E.; Homola, J. Copolymer Brush-Based Ultralow-Fouling Biorecognition Surface Platform for Food Safety. *Analytical Chemistry* **2016,** *88* (21), 10533-10539.
18. Chou, Y. N.; Sun, F.; Hung, H. C.; Jain, P.; Sinclair, A.; Zhang, P.; Bai, T.; Chang, Y.; Wen, T. C.; Yu, Q. M.; Jiang, S. Y. Ultra-low fouling and high antibody loading zwitterionic hydrogel coatings for sensing and detection in complex media. *Acta Biomater.* **2016,** *40*, 31-37.
19. Vaisocherová-Lísalová, H.; Víšová, I.; Ermini, M. L.; Špringer, T.; Song, X. C.; Mrázek, J.; Lamačová, J.; Scott Lynn, N.; Šedivák, P.; Homola, J. Low-fouling surface plasmon resonance biosensor for multi-step detection of foodborne bacterial pathogens in complex food samples. *Biosensors and Bioelectronics* **2016,** *80*, 84-90.
20. Riedel, T.; Hageneder, S.; Surman, F.; Pop-Georgievski, O.; Noehammer, C.; Hofner, M.; Brynda, E.; Rodriguez-Emmenegger, C.; Dostálek, J. Plasmonic Hepatitis B Biosensor for the Analysis of Clinical Saliva. *Analytical Chemistry* **2017,** *89* (5), 2972-2977.
21. Leng, C.; Huang, H.; Zhang, K.; Hung, H. C.; Xu, Y.; Li, Y.; Jiang, S.; Chen, Z. Effect of Surface Hydration on Antifouling Properties of Mixed Charged Polymers. *Langmuir* **2018,** *34* (22), 6538-6545.
22. Schlenoff, J. B. Zwitteration: coating surfaces with zwitterionic functionality to reduce nonspecific adsorption. *Langmuir : the ACS journal of surfaces and colloids* **2014,** *30* (32), 9625-9636.
23. Leng, C.; Sun, S.; Zhang, K.; Jiang, S.; Chen, Z. Molecular level studies on interfacial hydration of zwitterionic and other antifouling polymers in situ. *Acta Biomater* **2016,** *40*, 6-15.
24. Chen, S.; Li, L.; Zhao, C.; Zheng, J. Surface hydration: Principles and applications toward low-fouling/nonfouling biomaterials. *Polymer* **2010,** *51* (23), 5283-5293.
25. Herrwerth, S.; Eck, W.; Reinhardt, S.; Grunze, M. Factors that Determine the Protein Resistance of Oligoether Self-Assembled Monolayers − Internal Hydrophilicity, Terminal Hydrophilicity, and Lateral Packing Density. *Journal of the American Chemical Society* **2003,** *125* (31), 9359-9366.
26. Zhao, C.; Li, L.; Wang, Q.; Yu, Q.; Zheng, J. Effect of Film Thickness on the Antifouling Performance of Poly(hydroxy-functional methacrylates) Grafted Surfaces. *Langmuir* **2011,** *27* (8), 4906 - 4913.
27. Brault, N. D.; Sundaram, H. S.; Li, Y.; Huang, C.-J.; Yu, Q.; Jiang, S. Dry Film Refractive Index as an Important Parameter for Ultra-Low Fouling Surface Coatings. *Biomacromolecules* **2012,** *13* (3), 589-593.
28. Ogieglo, W.; Wormeester, H.; Eichhorn, K.-J.; Wessling, M.; Benes, N. E. In situ ellipsometry studies on swelling of thin polymer films: A review. *Progress in Polymer Science* **2015,** *42*, 42-78.
29. Blackman, L. D.; Gunatillake, P. A.; Cass, P.; Locock, K. E. S. An introduction to zwitterionic polymer behavior and applications in solution and at surfaces. *Chemical Society Reviews* **2019,** *48* (3), 757-770.
30. Leng, C.; Han, X.; Shao, Q.; Zhu, Y.; Li, Y.; Jiang, S.; Chen, Z. In Situ Probing of the Surface Hydration of Zwitterionic Polymer Brushes: Structural and Environmental Effects. *The Journal of Physical Chemistry C* **2014,** *118* (29), 15840-15845.
31. Yang, J.; Chen, H.; Xiao, S.; Shen, M.; Chen, F.; Fan, P.; Zhong, M.; Zheng, J. Salt-Responsive Zwitterionic Polymer Brushes with Tunable Friction and Antifouling Properties. *Langmuir* **2015,** *31* (33), 9125-9133.
32. Arwin, H. Ellipsometry in Life Sciences. In *Handbook of Ellipsometry*, Tompkins, H. G.; Irene, E. A., Eds.; William Andrew Publishing: Norwich, NY, 2005, 799-855.
33. Farka, Z.; Kovar, D.; Skladal, P. Rapid detection of microorganisms based on active and passive modes of QCM. *Sensors (Basel, Switzerland)* **2014,** *15* (1), 79-92.
34. Homola, J. *Surface Plasmon Resonance Based Sensors*; Springer-Verlag2006; Vol. 4. p 251.
35. Bittrich, E.; Burkert, S.; Müller, M.; Eichhorn, K.-J.; Stamm, M.; Uhlmann, P. Temperature-Sensitive Swelling of Poly(N-isopropylacrylamide) Brushes with Low Molecular Weight and Grafting Density. *Langmuir* **2012,** *28* (7), 3439-3448.
36. Kroning, A.; Furchner, A.; Aulich, D.; Bittrich, E.; Rauch, S.; Uhlmann, P.; Eichhorn, K.-J.; Seeber, M.; Luzinov, I.; Kilbey, S. M.; Lokitz, B. S.; Minko, S.; Hinrichs, K. In Situ Infrared Ellipsometry for Protein Adsorption Studies on Ultrathin Smart Polymer Brushes in Aqueous Environment. *ACS Applied Materials & Interfaces* **2015,** *7* (23), 12430-12439.
37. Tang, Y.; Lu, J. R.; Lewis, A. L.; Vick, T. A.; Stratford, P. W. Swelling of Zwitterionic Polymer Films Characterized by Spectroscopic Ellipsometry. *Macromolecules* **2001,** *34* (25), 8768-8776.
38. Furchner, A.; Bittrich, E.; Uhlmann, P.; Eichhorn, K. J.; Hinrichs, K. In-situ characterization of the temperature-sensitive swelling behavior of poly(N-isopropylacrylamide) brushes by infrared and visible ellipsometry. *Thin Solid Films* **2013,** *541*, 41-45.
39. Zhang, Z.; Vaisocherová, H.; Cheng, G.; Yang, W.; Xue, H.; Jiang, S. Nonfouling Behavior of Polycarboxybetaine-Grafted Surfaces: Structural and Environmental Effects. *Biomacromolecules* **2008,** *9* (10), 2686-2692.
40. Zheng, J.; Li, L.; Tsao, H. K.; Sheng, Y. J.; Chen, S.; Jiang, S. Strong repulsive forces between protein and oligo (ethylene glycol) self-assembled monolayers: A molecular simulation study. *Biophysical Journal* **2005,** *89* (1), 158-166.
41. Rodriguez Emmenegger, C.; Brynda, E.; Riedel, T.; Sedlakova, Z.; Houska, M.; Alles, A. B. Interaction of blood plasma with antifouling surfaces. *Langmuir* **2009,** *25* (11), 6328-33.
42. Vaisocherova, H.; Brynda, E.; Homola, J. Functionalizable low-fouling coatings for label-free biosensing in complex biological media: advances and applications. *Analytical and bioanalytical chemistry* **2015**, 407(14), 3927-3953.